Science of the Total Environment 642 (2018) 77–89

Contents lists available at ScienceDirect

Science of the Total Environment

journal homepage: www.elsevier.com/locate/scitotenv

Integrated interrogation of causes of membrane fouling in a pilot-scale anoxic-oxic membrane bioreactor treating oil refinery wastewater

Olusegun K. Abass [a,b], Fang Fang [a], Maoshui Zhuo [a,b], Kaisong Zhang [a,*]

[a] CAS Key Laboratory of Urban Pollutant Conversion, Institute of Urban Environment, Chinese Academy of Sciences, Xiamen 361021, China
[b] University of Chinese Academy of Sciences, Beijing 100049, PR China

HIGHLIGHTS

- Advanced chemical and Illumina sequencing unveils key MBR foulants in ORW treatment.
- Less biodegradable hydrocarbon and organophosphonate groups are key MBR foulants.
- Emulsified oil with mean sizes >0.5 μm are potential membrane foulants in the MBR.
- Bio-colonization of membrane surface in the MBR is a result of species sorting.

GRAPHICAL ABSTRACT

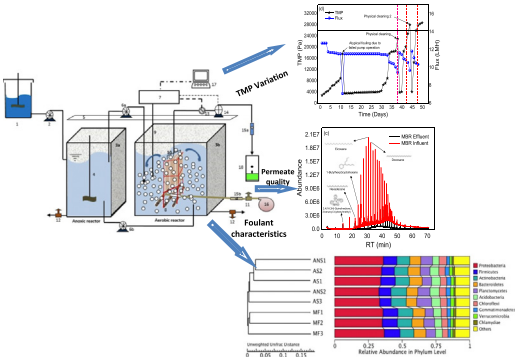

ARTICLE INFO

Article history:
Received 8 April 2018
Received in revised form 3 June 2018
Accepted 4 June 2018
Available online 9 June 2018

Editor: Zhen (Jason He)

Keywords:
Emulsified oil
Illumina sequencing
Membrane bioreactor
Membrane fouling
Microbial community
Oil refinery wastewater

ABSTRACT

Studies on membrane fouling during treatment of oil refinery wastewater (ORW) via membrane bioreactor (MBR) are currently lacking, and associated fouling challenges are largely undocumented. Using advanced chemical and Illumina sequencing approach, we investigated the complex bio-physiochemical interactions responsible for foulant-membrane interactions during treatment of ORW. After nearly 2 months of the MBR operation, COD removal reached maximal of 97.15 ± 1.85%, while oil and grease removal was maintained at 96.6 ± 2.6%, during the treatment duration. Most of the less or non-biodegradable oil moieties (>0.5 μm) progressively accumulated on the membrane as the influent oil concentration increased. Presence of relatively higher unsaturated extracellular polymers (100.6 mg/g VSS) like fulvic acid and aromatic-like compounds at high volumetric loading (~18.7 kg COD/m^3/d), enhanced the adsorption of chemical elements (Fe = 88.9, Al = 63.4, and Ce = 0.56 mg/g dry-sludge, respectively). Moreover, shift in microbial community structure to hydrocarbon-utilizing and metals-tolerating genera, as *Comamonas* and *Rhodanobacter*, respectively, uncovers major membrane colonizers in ORW treatment via MBR.

1. Introduction

The global demand of crude oil and natural gas in modern day industrialization is ever increasing. However, like most production activities, natural gas and oil production processes generate large streams of wastewaters. These wastewaters are derived from a number of crude oil and gas drilling and refining activities, which results in streams of varied organic and inorganic compositions and concentrations with potent capabilities to migrate downstream to pollute groundwater, or spill into surface waters causing large-scale environmental disturbances (Fakhru'l-Razi et al., 2009). In particular, oil refinery wastewaters

* Corresponding author.
E-mail address: kszhang@iue.ac.cn (K. Zhang).

https://doi.org/10.1016/j.scitotenv.2018.06.049
0048-9697/

(ORW) contains varied class of pollutants such as oil, dissolved solids, phenols, sulfides, and toxic metals, which encumbers available treatment facilities and thus, makes this class of wastewaters very challenging to treat via conventional methods (Santos et al., 2016).

The vast prospect in membrane bioreactor (MBR) applications for remediation of different class of industrial wastewater matrices including ORW has been identified (Rahman and Al-Malack, 2006; Razavi and Miri, 2015; Yu et al., 2018). However, a major drawback associated with MBR treatment of ORW is membrane fouling (Abass et al., 2015; Munirasu et al., 2016; Padaki et al., 2015). These drawbacks are intricately tied to different factors including the complex biology (activated sludge and biofilms), chemicals (influent characteristics and inorganic elements), materials (membrane type and characteristics), and processes (operating conditions and reactor properties) affecting the sustained long-term treatment of ORW in MBR systems (Lin et al., 2011; Padaki et al., 2015; Qin et al., 2015; Shariati et al., 2011; Viero et al., 2008).

For instance, Viero et al. (2008), investigated the effect of high organic load in a submerged MBR (SMBR) treating oil refinery wastewater during long-term operation and observed that modification of the feed characteristics resulted in increased production of polysaccharide fractions, which aggravated the membrane permeability. However, the interaction leading to the membrane performance degradation was less explored. In another report by Rahman and Al-Malack (2006), a laboratory scale cross-flow MBR was utilized for the treatment of petroleum refinery wastewater, which showed good COD removal efficiency of over 93%. However, information regarding membrane fouling were scantly discussed. More recently, Razavi and Miri (2015) explored the treatment of real petroleum refinery wastewater (PRW) in a hollow fiber MBR. Details on the MBR treatment performance and sludge characteristics were reported, but the membrane fouling characteristics of the real PRW were less examined.

Similarly, Shariati et al. (2011) focused mainly on the effect of hydraulic retention time (HRT) in relation to its impact on extracellular polymeric substances (EPS) and soluble microbial products (SMP) production, and the accompanying fouling implications. Increased contributions on fouling characteristics and control were made by Pajoumshariati et al. (2017) and Qin et al. (2015), where they both utilize physical and chemical method to investigate fouling development and control during treatment of PWR/oily wastewater in membrane sequencing batch reactors (MSBR) and SMBR, respectively. However, information regarding chemical and biological interactions in relation to the fouling propensity of the membrane were lacking in the study. Thus, the evident shortage of research on the complex causes of fouling in MBR systems treating ORW can potentially hamper the promising prospect of MBR for ORW remediation and reuse.

Therefore, studies that seek to understand membrane fouling development in MBR applications treating ORW are urgently needed. Accordingly, this paper aims to interrogate via an integrated approach the complex physical, chemical and biological interactions responsible for membrane fouling during treatment of ORW in MBR. Findings on the influent compositional characteristics and its influence on membrane fouling were made. The inextricable links between chemical foulants and bio-products were discussed, and finally, we showed via high-throughput sequencing the microbial distribution and structure of membrane colonizers during treatment of oil refinery wastewaters in MBR systems.

2. Materials and methods

2.1. Pilot scale anoxic-oxic MBR design and operation

The pilot scale anoxic-oxic MBR (A/O-MBR) plant was built at the Urban Pollution Conversion Centre of the Institute of Urban Environment, Xiamen as shown in the Fig. 1. Other design characteristics of the MBR setup, membrane type and operating parameters are presented in Table 1. The model wastewater samples based on oil-refinery effluent (Alexandre et al., 2016) were prepared by emulsifying a mixture of motor oil (Shengao, China) and Phenol (Sinopharm Chemical Reagent Co. Ltd., China) with Pluronic F-127 (Sigma Aldrich, USA), which serves two purposes; emulsification of the oil molecules, and to reduce coalescence in the MBR sludge, thereby enabling higher cells oxygen contact (Alexandre et al., 2016). Mean sizes and zeta-potential of the oil-in-water emulsions were characterized using Zetasizer (Nano ZS, Malvern). The synthetic wastewater was augmented with essential nutrients (including NH_4Cl, KH_2PO_4, $CaCl_2.2H_2O$, $NaHCO_3$, $MgSO_4.7H_2O$, $CoCl_2.6H_2O$, $FeCl_3$, and $MnSO_4$ in proper amounts) to aid microbial activity and the A/O-MBR was operated at volumetric loading of ~1.6 kg COD/m^3/d to ~18.7 kg COD/m^3/d for about 2 months to mimic periods of low and high volumetric loading rates. The reactors were operated under low volumetric loading for 20 days at 1.6 to 2.5 kg COD/m^3/d and under high volumetric loading for 30 days at 5.9 to 18.7 kg COD/m^3/d. Physical cleaning only (to ensure that natural surface environment of the membrane is preserved to meet the experimental aim) were performed, as the transmembrane pressure increased to 23 kPa and 28 kPa, respectively.

2.2. Sampling and analysis

Influent and effluent water samples were collected from the A/O-MBR set-up daily and weekly for COD, oil and grease (O&G) analyses, respectively. Concentrations and compositions of O&G were quantified using standard gravimetric method (USEPA, 2009) and gas chromatography–mass spectrometry (GC–MS) investigation, respectively (Abass et al., 2017). Procedure for the O&G sample extraction is described in the Supporting information (SI). Other physicochemical indices such as COD, TOC, MLSS, MLVSS and TDS were measured in accordance with Standard Methods for the Examination of Water and Wastewater (APHA, 2005).

Triplicate samples of 10 g each, mixed liquor (anoxic and oxic) and membrane foulant were retrieved during physical cleaning (PC) episodes corresponding to TMP jumps (on Day 11, 37 and 50) for chemical, spectroscopic and microbial community analysis. Foulant samples were collected by scrapping off the sludge cake along with the thin gel layer using plastic collectors at different times corresponding to the cleaning periods. The membrane surface was subsequently flushed with tap water and re-inserted in the MBR module for further use. All samples collected for DNA extraction were immediately frozen under sub-zero temperature (−20 °C).

2.3. Spectroscopic and chemical analysis of mixed liquor and foulant components

SMP and EPS were extracted from the A/O-MBR mixed liquor and foulant layer using heat treatment method as described by Zhang et al. (2011). Briefly, harvested samples were centrifuged at 7000 rpm (at 4 °C) for 10 min, followed by filtration of 3 mL of the supernatant through a 0.22 μm PTFE membrane. The resulting filtrate represents the SMPs. Subsequently, the dewatered pellet was washed and re-suspended to its initial volume using a buffer solution (165 mM Phosphate-buffered saline – 1.094 g Na_2HPO_4, 0.277 g NaH_2PO_4 and 8.476 g NaCl, at pH 7.2), and mixed for 10 min. The resulting mixed liquor was heat treated at 80 °C for 10 min, and centrifuged at 10,000 rpm at 4 °C for 10 min. The recovered filtrate after centrifugation was regarded as the EPS. The Anthrone sulfuric method (Koehler, 1952) and the modified Bradford method (López et al., 1993) were used for determination of the polysaccharides and proteins fractions, respectively. Three-dimensional fluorescence excitation-emission matrix (EEM) spectral fingerprints of the foulant and bulk sludge supernatant samples (filtered through a 0.45 μm cellulose membrane) were collected using luminescence spectrometry (F-4600 FL spectrophotometer, Hitachi, Japan) as described by Wang et al. (2010). Origin Pro 9.0 software

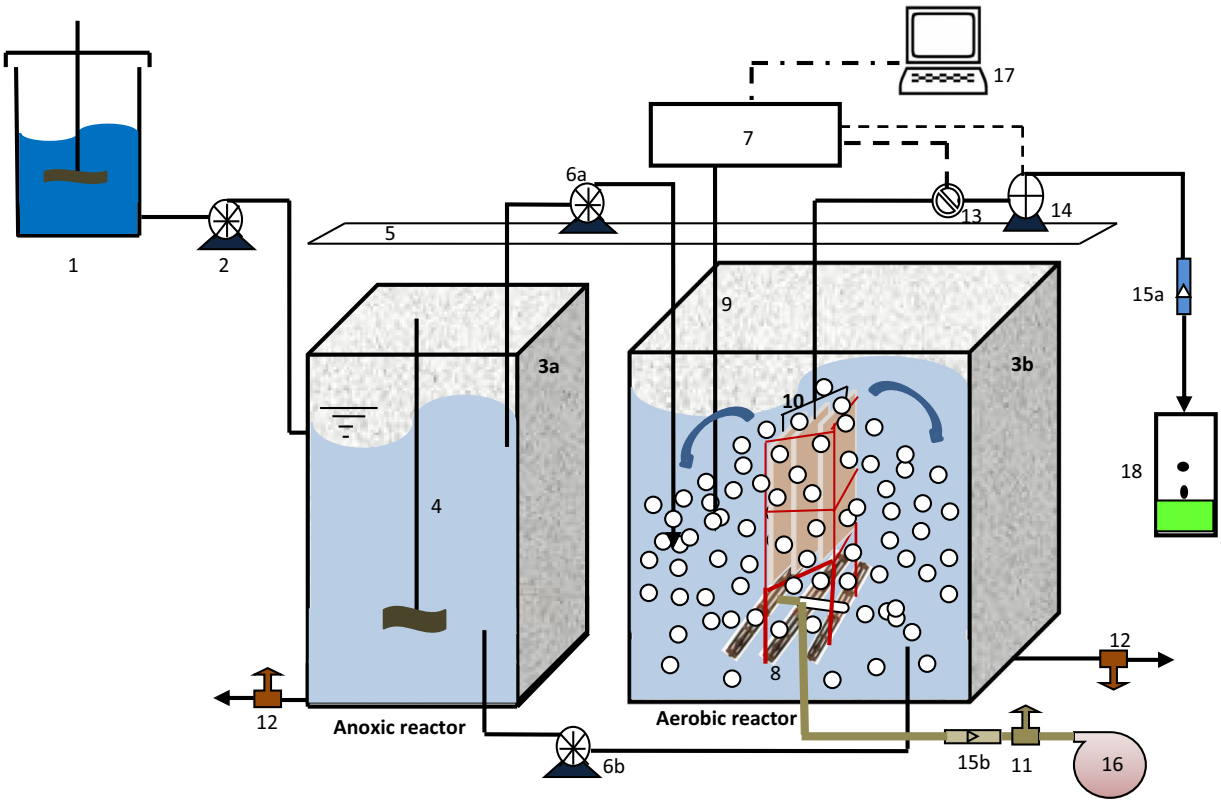

Fig. 1. Schematic design of the anoxic-aerobic MBR Set-up (1. Feed tank 2. Influent peristaltic pump 3(a&b). Anoxic and aerobic tank 4. Sludge mixer 5. Installation support 6 (a&b). MBR influent pump and recirculation pump 7. Automation control box 8. Air sparger 9. pH probe 10. Flat sheet membrane module (3pieces arranged in parallel) 11. Fluid control valves 12. Sludge discharge valve 13. Pressure transducer 14. Suction (permeate) pump 15. (a&b). Water and air flow meter 16. Air pump 17. Computer detection 18. Permeate tank).

(Origin Lab Corporation, USA) was employed for handling the EEM data and a novel 3-D EEM spectra plot with X and Y axis (scaled from 0 to 10) representing the emission and excitation spectra, respectively and a *Z*-axis, which represents the fluorescence intensity (FI) was used.

X-ray fluorescence spectroscopy (XRF) was used for the qualitative and quantitative analysis of the inorganic components of the MBR bulk sludge and foulant layer on Day 50. The analysis was carried out on a ZB Axios-mAX spectrometer as described by Abass et al. (2017). Similarly, both samples retrieved on the same day as the XRF samples were subjected to Fourier transform infrared (FTIR) measurement to investigate the organic components using FTIR spectrophotometer (Nicolet iS10, Thermo Scientific, USA). Both the sample preparation and instrument limit of determination methods are described in Abass et al. (2017).

2.4. DNA extraction and PCR amplification

0.5 g-pelleted samples of the mixed liquor (anoxic and oxic) and membrane foulant were used for the DNA extraction employing FastDNA-SPIN kit for Soil (MP-Bio, Santa Ana, CA, USA), following the manufacturer's prescribed protocol. The concentration and quality of the genomic DNA were determined by micro-spectrophotometric technique using NanoDrop ND-1000 (NanoDrop Technologies, Willmington, DE, USA). Further, the V4 region of 16S rRNA genes were selected for PCR amplification using the bacterial and archeal primers set 515F (GTGCCAGCMGCCGCGGTAA), U519F (CAGYMGCCRCGGKAAHACC), and 806R (GGACTACHVGGGTWTCTAAT). All PCR reactions were carried out in 30 μL reactions with 15 μL of Phusion® High-Fidelity PCR Master Mix (New England Biolabs); 0.2 μM of forward and reverse primers, and

Table 1
Operating conditions of the A/O-MBR set-up and membrane characteristics during startup operation.

Operating parameter	Measurement	Membrane characteristics	Measurements
Total HRT (h)	17.4	Effective membrane surface area (m^2)	0.8054
Membrane Flux (LMH)	12.7	Nominal pore size (μm)	0.15
Anoxic tank HRT (h)	4.7	Membrane contact angle	75
Aerobic tank HRT (h)	10	Membrane type	MF
Anoxic DO (mg/l)	0.35	Membrane material	PVDF
Aerobic DO (mg/l)	5.12	Membrane configuration	Flat Sheet
Temperature (°C)	22.7 ± 2.0	Permeate operation mode	On: 10mins, Idle: 2mins
SRT (Days)	35	No. of membrane unit	3
Mixer speed (rpm)	150		
Anoxic working volume (L)	40		
Aerobic working volume (L)	102.4		
Aerobic sludge MLSS/MVLSS (mg/L)	6720–7345/3230–3850		
Anoxic sludge MLSS/MVLSS (mg/L)	8310–9005/4170–4650		
Recirculation flow ratio	2:1		
pH in anoxic/aerobic tank	7.1 ± 0.2/7.5 ± 0.5		
Viscosity of Mixed liquor (mPa·s)	6.0		

about 10 ng template DNA. The thermal cycling consisted of initial denaturation at 98 °C for 1 min, followed by 30 cycles of denaturation at 98 °C for 10 s, and primer annealing 50 °C for 30 s, and elongation at 72 °C for 30 s, and a final step at 72 °C for 5 min. The PCR products were analyzed by gel electrophoresis using 2% (w/v) agarose gel in a 1× TAE buffer (containing SYB green). Samples with bright main strip between 400 and 450 bp were chosen for further experiments.

2.4.1. High-throughput sequencing of 16S rRNA gene amplicons

The PCR products were mixed in equidensity ratios and purified with GeneJET Gel Extraction Kit (Thermo Scientific) and libraries were generated using Illumina TruSeq DNA PCR-Free Library Preparation Kit (Illumina, USA) following manufacturer's recommendations, and index codes were added. The library quality was assessed on the Qubit@ 2.0 Fluorometer (Thermo Scientific) and Agilent Bioanalyzer 2100 system. Eventually, the library was sequenced on an Illumina HiSeq 2500 platform (Novogene, Beijing, China), and 250 bp paired-end reads were generated.

2.4.2. Biodiversity analysis and community structure

Paired-end reads from the original DNA fragments were merged using FLASH (Magoc and Salzberg, 2011), and assigned to each sample according to the unique barcodes. The sequencing data were analyzed using QIIME (Caporaso et al., 2010) software package (Quantitative Insights Into Microbial Ecology), and in-house Perl scripts were used to analyze alpha and beta diversities. Afterward, the pick_de_novo_otus.py was used to pick operational taxonomic units (OTUs) by making OTU table. Sequences with ≥97% similarity were assigned to the same OTUs. Representative sequences for each OTU were picked and the RDP (Ribosomal Database Project) classifier (Wang et al., 2007) were used to annotate taxonomic information for each representative sequence. To avoid the effect of variation among replicates and to counterbalance stochastic sampling efforts, the triplicate samples were merged together to form OTU profiles, emerging into 8 pooled samples. The OUT table was further clustered into anoxic sludge (ANS2–1), MBR sludge (AS3–1), and membrane foulants (MF3–1) based on biomass component and sampling dates, i.e. early MF3, AS3 and ANS2 (Day 11), middle MF2, AS2 and ANS1 (Day 37), and late MF1 and AS1 (Day 50) (Table S1). Further, clustered heatmaps (R version 3.2.5) were used to visualize the shared genera and the distribution of the various bacterial phyla and classes within each sample subsets.

In order to compute Alpha diversity, we rarify the OTU table and calculate four metrics: Chao1, ACE, Observed Species, and the Shannon index. Simpson's index was also computed. Unweighted Uni-Frac distance for the membrane foulants and mixed liquor samples was calculated based on the categories above, and subsequently visualized by nonmetric multidimensional scaling (NMDS). The unweighted pair group method with arithmetic mean (UPGMA) was used for the sample clustering. Reproducibility and differences between the samples were measured using ANOSIM, which is a statistic test (R) having values ranging from 0 to 1 (where $R = 0$, means no similarity and $R = 1$, means dissimilarities in community structure).

3. Results and discussion

3.1. Performance of the anoxic-oxic MBR

Major characteristics of the model ORW oil/water emulsion are presented in the Table 2 and information regarding its suitability as ORW are detailed in SI. The influent COD concentrations were varied sharply to accommodate for the highly varied COD concentrations characteristic of oil refineries discharges, which is partly due to temporal or long-term shut down of petrochemical plants or plant malfunction (Di Fabio et al., 2013). This particularly holds true for countries in Asia (e.g. China), which has witness severe groundwater and surface water contamination events from petrochemical wastewater discharges (Xu et al., 1998). In the two-stage treatment process, the MLSS in the anoxic reactor was varied between 8.3 g/L and 9.0 g/L, and in the MBR, between 6.7 g/L and 7.3 g/L during the whole treatment duration. The A/O-MBR was steadily operated at constant flux of 12.7 LMH for nearly 2 months at total HRT of 17.4 h, which achieved overall stable COD removal efficiency of 95.3 ± 4.1% as shown in Fig. 2a. Prior to operation, the sludge biomass obtained from a local municipal wastewater treatment plant in Xiamen, China was acclimatized with the model oil refinery wastewater for three months as described by Ben-Youssef and Vazquez-Rodriguez (2011). In the 30th and 85th day of acclimatization, the supernatant COD values were 411.3 mg/L and 292.6 mg/L in the anoxic reactor, and 358 mg/L and 143.4 mg/L in the aerobic reactor, respectively, compared to the initial supernatant COD concentration of 802 mg/L after addition of the synthetic wastewater and essential nutrients.

Table 2
Characteristics of the model oil refinery wastewater.

Parameters	Measurements
Influent COD (mg/l)	603–7850
Phenol (mg/l)	5–43.9
Oil & Grease (mg/l)	16.7–260.4
TDS (mg/l)	588–715
Pluronic F-127 (mg/l)	1–8.13
Turbidity (NTU)	101.3–104
TOC (mg/l)	150.8–1962.5
Zeta potential (mV)	−38.2 to −33.8
Oil droplet mean size (nm)	375.9–767.3

The permeate COD concentration in the A/O-MBR varied between 28.4 and 60.8 mg/L during the whole period of treatment, when the influent COD concentrations fluctuated from 603.7 to 7866.5 mg/L. The COD volumetric loading was kept constant at 1.56 kg COD/m^3/d in the first 10 days. During this period, the permeate COD was 49 ± 9.0 mg/L. Afterwards, the COD volumetric loading was steadily increased from 2.46 kg COD/m^3/d to 18.72 kg COD/m^3/d. As earlier described, the influent COD was fluctuated in order to a) mimic the varied COD loading conditions in real applications; b) investigate the capacity of the MBR to reduce the COD load, and c) to study the effect of this loading condition on the membrane fouling correspondingly (Fig. 2a). Similarly, the overall O&G removal efficiency throughout the treatment duration range from 94% to 99.2% (Fig. 2b), while results from the GC–MS investigation showed that some of the organic compounds including 1 Butylhexyl cyclohexane, docosane, pentadecane, nonadecane were partially or completely degraded as seen in the effluent respectively on Day 46, compared to influent organic components (Fig. 2c). During the entire operation, the effluent O&G concentration (1.0 mg/L to 2.2 mg/L) remained below the national discharge standard (<10 mg/L) for oil wells and surface water, respectively. O&G removal in the MBR system may have resulted from adsorption the oil moieties on sludge particles as also reported by Yu et al. (2018), during the treatment of synthetic wastewater via MBR. In addition, membrane surface rejection of non-biodegradable colloidal oil moieties as discussed in Section 3.4 will contributed to the removal. However, higher removal of O&G is mainly due to native oil degrading microbes present in the sludge mixed liquor as described in Section 3.5. Similarly, Sarkar et al. (2017), observed that the presence of Proteobacteria genera derived from native oil refinery sludge could enhance the biodegradation capacity of hydrocarbon compounds. The most abundant bacteria group in the A/O-MBR sludge mixed liquor is the Proteobacteria group (see Section 3.5), which also shows the presence of Proteobacteria genera like *Comamonas*, with superior metabolic properties for polyaromatic and aliphatic hydrocarbon utilization. Yu et al. (2018) made similar findings after analysis of the microbial communities in three sets of MBRs at different SRTs.

The efficiency of the A/O MBR is comparably similar to those described by Rahman and Al-Malack (2006) where the cross-flow MBR

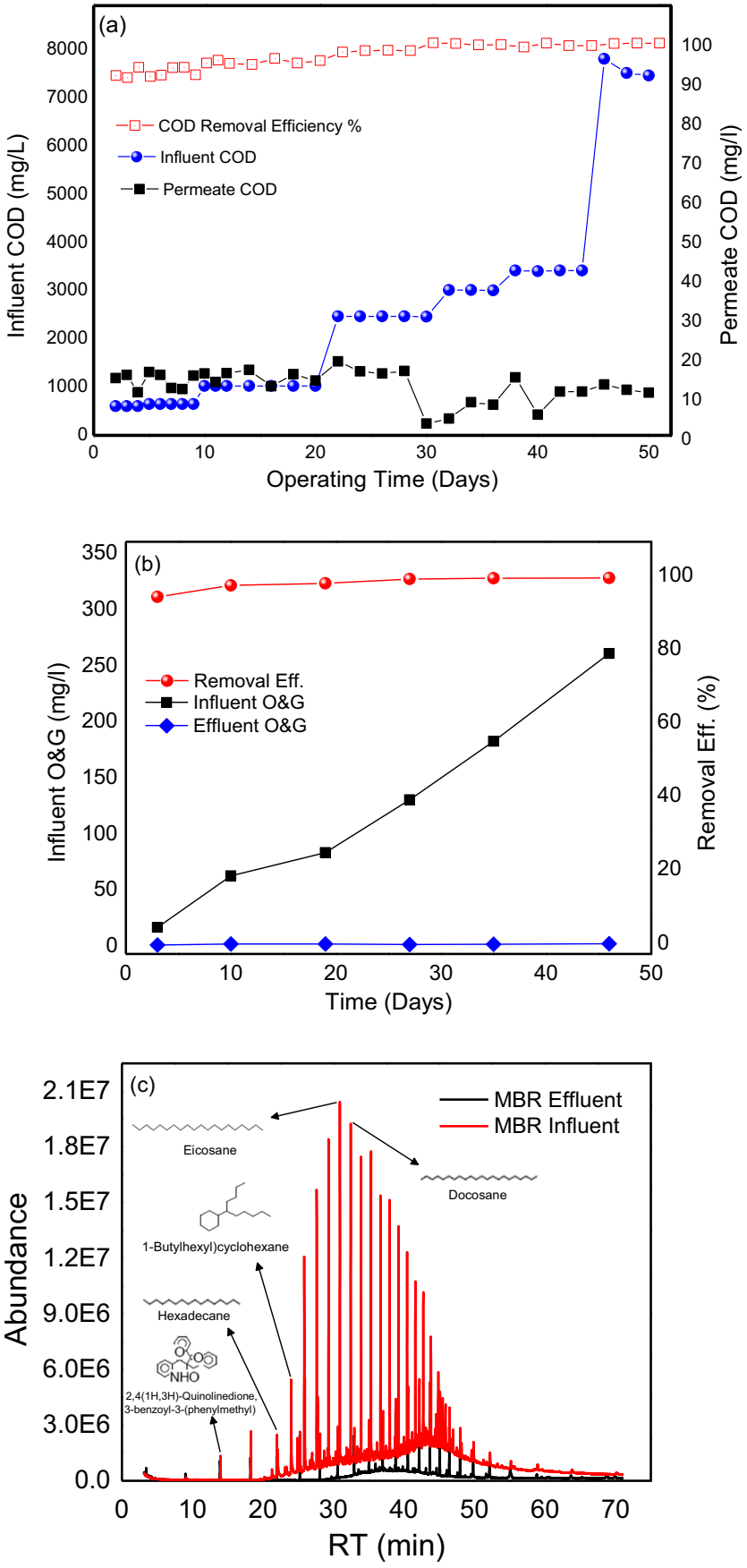

Fig. 2. Performance indicators of the pilot-scale anoxic-aerobic MBR for (a) COD removal (b) Oil and grease removal (c) total ion chromatogram of the MBR influent and effluent acquired in full scan mode on an Agilent GC–MS HP-5MS column.

utilized achieved COD removal >93%, at initial COD concentration >370 g/L (influent pumped intermittently for 2 min every 2 h) when treating oil refinery wastewater. However, in the work conducted by Viero et al. (2008), when the influent COD concentration was ~952 mg/L, the COD removal efficiency was 58%, which is relatively lower than the values reported in this work, and in previous study (Rahman and Al-Malack, 2006). The improved COD removal (95.3 to 99.0%) observed in this study may be as a result of the less complex nature of the synthetic ORW compared to those described by Viero et al. (2008), the microbial characteristics of the sludge mixed liquor and the first stage anoxic pretreatment of the wastewater, respectively.

3.2. Fouling propensity of the MBR system

The fouling tendency of the flat sheet membranes were directly monitored using the transmembrane pressure (TMP) variation, since the MBR was operated at constant flux throughout the experiment as shown in Fig. 3. Despite the nearly constant initial influent COD load (1.56 kg COD/m^3/d), the TMP values increased progressively from its initial value (2.8 kPa) after the MBR inoculation, to 8.8 kPa on Day 10. This is quite normal in most MBR plants as most part of the membrane surface are gradually colonized by colloidal materials, SMPs and EPS, microorganism and positively charged inorganic elements which have strong bonding affinities for negatively charged functional groups such as the carboxyl groups formed on the membrane surface (Hong et al., 2014; Lin et al., 2011). Unexpectedly, an atypical sharp rise in TMP (17.6 kPa) was witnessed on Day 11, which was due to failed MBR influent pump. Consequently, this led to a fall in the wastewater level and thus, exposed the membrane surface to the atmosphere while the suction pump was still in operation. This fouling abnormality was rectified by physically cleaning the membrane with fresh tap water to restore the membrane permeability. Though the cleaning operation was effective to restore the MBR flux to the prior value before the accidental fouling, it was unable to reach the initial flux, set at the start-up operation. Therefore, to achieve smooth, efficient and extended use of membranes in MBR, it is suggested that pumps equipped with sensors and capable of early detection of malfunctions should be used during MBR operation. Moreover, a gradual but stable build-up in TMP was observed from Day 12 to 32, before a sloppy jump in TMP, which occurred on Day 35. Despite the step-wise increment of COD load from 2.46 kg COD/m^3/d to 7.22 kg COD/m^3/d, the slow TMP growth seen in the MBR could be attributed to hydrodynamic control measures (including suction relaxation, air-scouring pressure, membrane unit spacing effect) adapted in the study as previously described in the literature (Abass et al., 2015; Wu et al., 2008), and anti-fouling properties of the PVDF membrane as shown in Table 1.

On Day 37, the flux dropped to the lowest value at 9.4 LMH, corresponding to TMP value of 23 kPa. Therefore, PC procedure was carried and operation continued afterward. Although, the PC operation helped regain the flux, it was not sustainable as the fouling heightened after few days (partly due to increased volumetric COD loading 8.18 kg COD/m^3/d), which necessitated a second PC procedure. As expected, the TMP declined and the flux recovered to the operating range. However, this was short-lived as the volumetric loading was increased to ~18.7 kg COD/m^3/d. The high volumetric shock loading from Day 19 to 45 (5.92 to 18.7 kg COD/m^3/d) might have induced a negative effect on the bacteria consortium leading to the increased production of extracellular polymers and dissolved microbial products (as discussed in Sections 3.3 and 3.5), which has been confirmed to be closely related to TMP jump in MBR applications (Meng et al., 2017).

Similarly, increase in O&G concentration from 83.3 mg/L, on Day 19 to 260.4 mg/L on Day 45 (Fig. 3), is a key contributing factor to the accelerated fouling of the membrane despite the repeated PC operation performed (Fig. 3). Previously, Shariati et al. (2011) speculated that organic compounds were main component of membrane pore fouling during treatment of PWR using MSBR. To confirm this, analysis of the oil droplet mean sizes was performed, and results showed that the mean oil droplet size ranged from 0.376 μm to 0.767 μm, whereas, the mean pore diameter of the MF membrane was 0.15 μm (Tables 1 and 2). Hence, it is probable that majority of the non-biodegradable colloidal oil particles were rejected at the membrane interface leading to increased fouling susceptibility of the membrane (see Section 3.4). In future applications, the use of coagulation-flocculation pretreatment (Santo et al., 2012), or an extended HRT could be adopted in the anoxic compartment, or the use of anaerobic degraders like up-flow anaerobic sludge blanket (Wang et al., 2016) could be effective to prolonging the membrane fouling propensity and therefore, achieving membrane longevity. Other oil-water emulsion pre-treatment technology that can be adopted include electrocoagulation technology (An et al., 2017) and porous materials like polyurethane foam, glass wool and Birch bark (Golub and Piekutin, 2018).

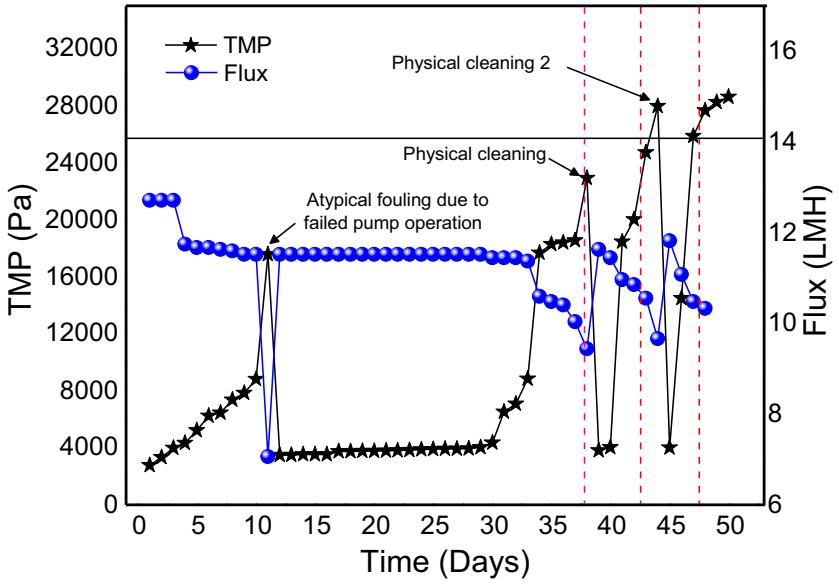

Fig. 3. Flux and TMP operation showing fouling propensity of the MBR under constant flux operation mode.

3.3. SMP and EPS compositional characteristics of the MBR system

Concentration and composition of SMP and EPS in bulk sludge and membrane cake layer has been directly associated with various causes of membrane fouling, including pore blocking and gel filtration resistance, respectively (Lin et al., 2011). In this study, analysis of the SMP and EPS in the bulk sludge and membrane foulant layer was conducted during episode of physical cleaning corresponding to Days 10 (used as control in relation to subsequent fouling episodes), 37 and 50, respectively. Fig. 4a shows the association between these bio-fractions and their components as found in the bulk sludge and membrane foulant layer represented in mg/g VSS of mixed liquor.

Interestingly, accumulation of SMPs (17.7 mg/g VSS) and EPS (28.7 mg/g VSS) on the membrane as seen on Day 37 were markedly high compared to the initial start-up concentrations (9.0 mg/g VSS and 10.2 mg/g VSS, respectively), which correlates well to the duration when the TMP build up was observed (Fig. 4a). It was earlier proposed that the early formation of a gelation layer in MBR generally within <15 days of start-up operation occur as a result of increased production of SMP (Hong et al., 2014). A more recent study however, suggested that colonization of the membrane surface by polysaccharide (due to their larger sizes and gelling properties) is mainly the culprit for the increased filtration resistance which is accompanied by a jump in TMP (Chen et al., 2016). In the current study, the SMP polysaccharide fractions increased from 3.0 mg/g VSS as observed on Day 11 to 20.8 mg/g VSS on Day 37, which implies that polysaccharide fractions are key membrane foulants in ORW treatment via MBR. However, interaction of divalent and multivalent cations (sourced from the MBR influent) with polysaccharide compounds could aggravate the filtration resistance via formation of impervious gels on the membrane surface as shown in Fig. 4b&c.

Similarly, as the influent loading rate increased (8.18 to 18.7 kg COD/m^3/d), both the SMP and EPS polysaccharide fractions of the fouled membrane surface increased progressively from Day 37 (34.8 mg/g VSS) to Day 50 (53.8 mg/g VSS) and were significantly higher than the protein fractions (11.5 mg/g VSS and 46.8 mg/g VSS respectively). This findings is consistent with previous study (Xin et al., 2015), and relatively confirms that polysaccharide compounds are key causes of fouling problems in MBR applications relative to the influent characteristics. The build-up of polysaccharide (53.8 mg/g VSS) on the membrane at Day 50, compared to the amount observed in the bulk sludge (20.3 mg/g VSS) verifies that a complex interaction of polysaccharide compounds via hydrophobic interaction, hydrogen bond and electrostatic interaction exist (Xu et al., 2013) as later discussed in Section 3.4. Hydrocarbon compounds adsorbed in the complex polysaccharide networks could be degraded by bacterial enzymes in the EPS (Sarkar et al., 2017), providing energy for growth and proliferation of membrane-attached hydrocarbon degrading microorganisms (as discussed in Section 3.5) and thus, leading to serious fouling problems in MBR systems treating oil refinery wastewater.

3.4. Spectroscopic analytical results

The accumulation of fulvic acids (described below) on the membrane interface gave rise to complex interactions with chemical elements in the MBR system as shown in the XRF analysis of the bulk sludge and membrane foulant layer (Fig. 4b&c). This is because fulvic acid possesses two or more functional groups (like phenolate, hydroxyl, and carboxylate) capable of chelating with chemical elements that produces divalent/multivalent cations (e.g. Ca, Sr, Fe, Mg, Pb, Al, P, Ba, Cu,) in aqueous solutions (Volkov et al., 2017). For example, Sr is known to form stable complexes with humic acids in alkaline and neutral media, where their sorption by mineral matters is considerably inhibited but conversely favors sorption onto solid organic phases as in the case of humic acid (Yu et al., 2015). Similarly, strong and less reversible Sr adsorption has been observed in organic matters with higher aromatics carbon contents compared to carbohydrates (Boyer et al., 2018).

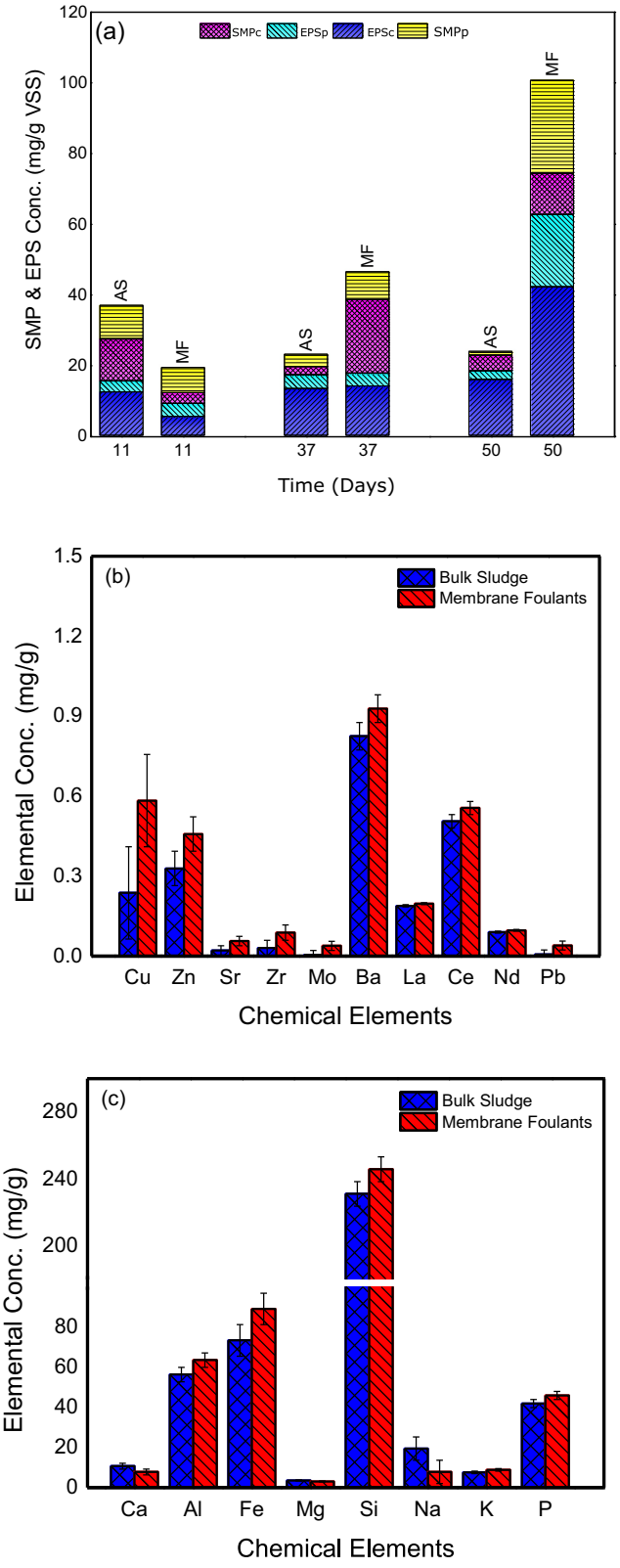

Fig. 4. Fouling associated components including (a) fractional concentrations of extracellular polymer and soluble microbial product in the MBR bulk sludge (AS) and membrane foulant (MF) during episode of TMP rise. (b) Mean composition and concentrations of minor elements and (c) major elements, found in the MBR bulk sludge (AS) and membrane foulant (MF) on Day 50.

Accumulation of chemical elements including Si, Fe, Al, Ba, Cu, Ce, Zn and Sr, in the membrane foulants at mean concentrations of 245.9, 88.9, 63.4, 0.93, 0.58, 0.56, 0.46, and 0.06 mg/g dry sludge, respectively was observed on Day 50. Compared to the membrane foulant, mean concentrations of chemical elements in the bulk sludge (Fig. 4b&c) were less, which indicates that adsorption of metals (initiated by presence of concentrated organics at the membrane surface) plays a key role in the membrane fouling process.

To further investigate the interactions of foulants on the membrane surface and bulk sludge, EEM analysis were carried out. Results reveals that the main membrane fouling component on Day 37 are soluble microbial products including tryptophan, tyrosine, and protein-like components (Wang et al., 2010), as demonstrated by the main peak at excitation/emission (Ex/Em) wavelengths of 290/355 nm (Fig. 5a). However, on Day 50, two major peaks at Ex/Em wavelengths of 220/440 and 225/335–280/330 were detected representing fulvic acid-like substances and aromatic protein, tryptophan-like material, or phenolic compounds with less degradable materials, respectively (Fig. 5b). The latter compounds mostly originate from the influent wastewater, as also documented by Wang et al. (2010). Furthermore, at Ex/Em wavelengths of 280/340 nm, 275/310 nm, and 285/345 nm, peaks characteristics of phenolic compounds, tyrosine, and tryptophan-protein-like soluble microbial products were dominantly found in the membrane foulants on Day 50, compared to the bulk sludge (on the same day) and membrane foulants on Day 37 (Fig. 5c&d). The membrane foulants component on Day 50 had similar characteristics variation with the influent wastewater, at increased volumetric loading.

Thus, as shown in Figs. 4b&c and 5, association of inorganic elements with organic components of the membrane foulant (mostly aromatic proteins, fulvic acid, phosphoric and carboxyl groups), are important pointers to the influence of wastewater influent composition on nature of fouling in MBR systems as also recently suggested by Wang et al. (2017). In addition, humid and fulvic acid can potentially bind artificial radionuclides (e.g. Zr, Ce, La, Nd) sourced from oil refinery wastewater as shown in Fig. 4b&c. Therefore, accumulation of rejected aromatic protein-like substances and fulvic acids at the membrane interface can give rise to a high degree of unsaturated EPS molecules (with low energetic barrier) and a network of metals complexes, which rapidly grow into macromolecules, and thus colonizing the membrane surface leading to fouling of the membrane.

Investigation of the functional groups and compositions of the bulk sludge and membrane foulant by means of FTIR analysis showed a broad-spectrum absorption from 3440 to 913 cm^{-1} (Fig. 6). The peaks are predominantly composed of O—H hydroxyl functional groups

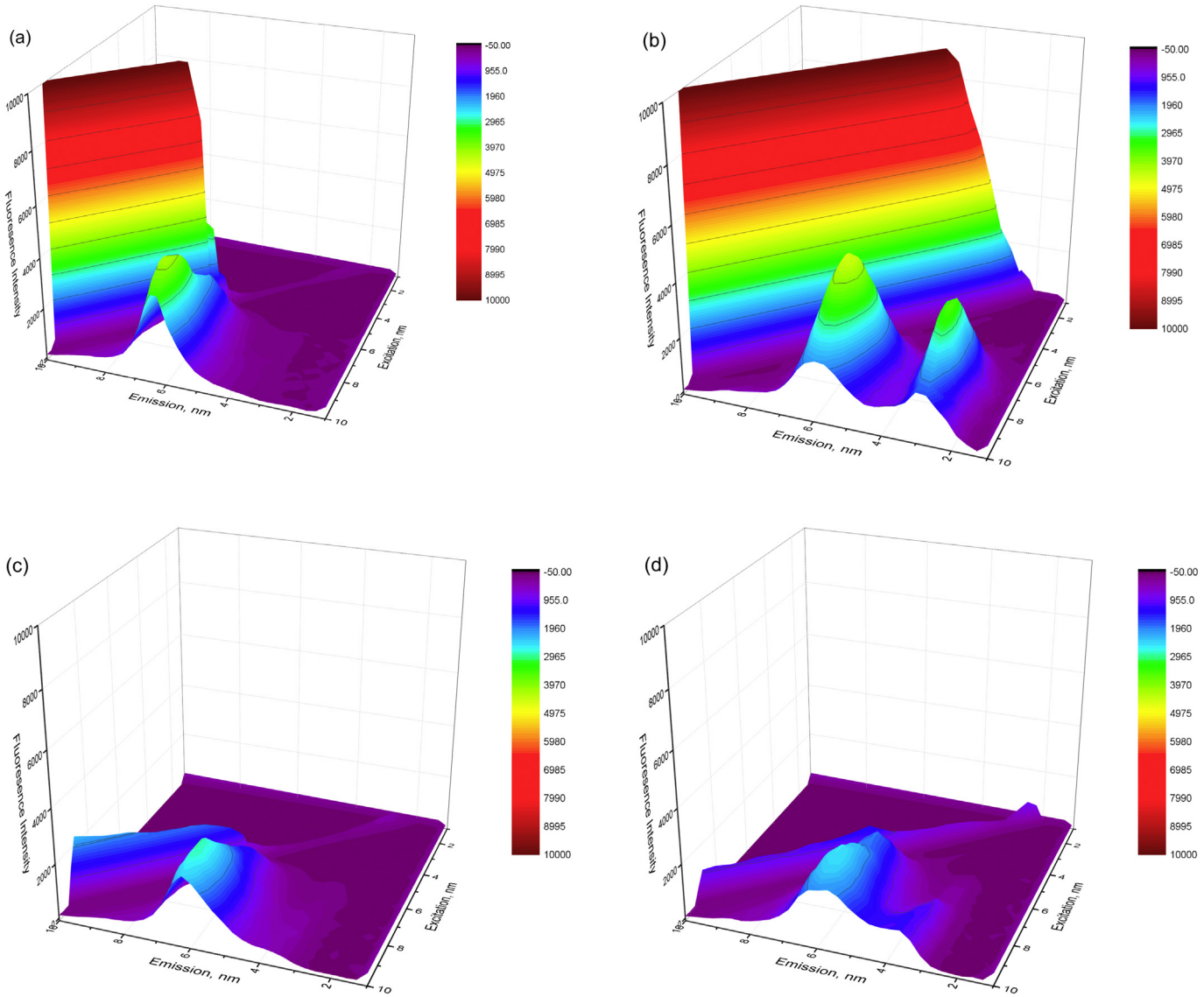

Fig. 5. Fluorescence excitation–emission matrix spectra of (a & b) membrane foulants on Day 37 and 50 (c&d) MBR bulk sludge on Day 37 and 50.

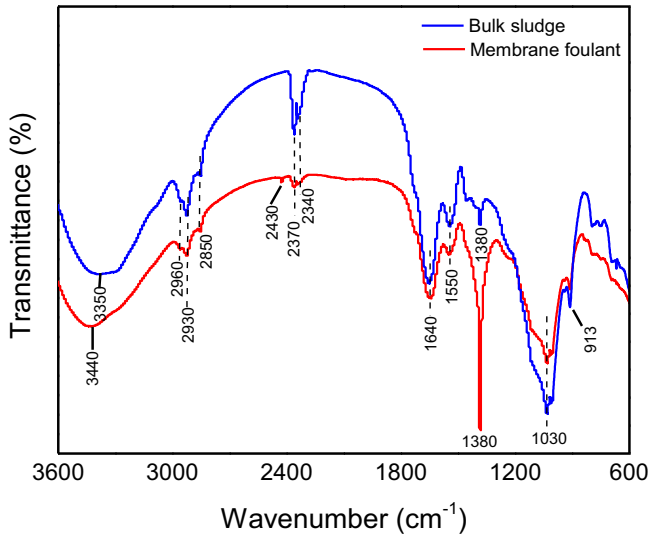

Fig. 6. Fourier transform infrared spectra of the bulk sludge and membrane foulant.

(including phenols and/or alcohols) (3350–3344 cm^{-1}) (Abass et al., 2017), symmetric and asymmetric C—H stretching vibration of alkanes (2960–2850 cm^{-1}) (Abass et al., 2017), N—H^+ stretching vibration of amine and imine hydrogen halides and an overlapping organophosphate group (2430–2340 cm^{-1}) (Socrates, 1980). The last set of peaks (1640–913 cm^{-1}) are generally related to EPS compositions including amide-protein related groups, carboxylic and hydrocarbon related groups, nuclei acid, and polysaccharide groups (Yuan et al., 2011).

Compared to the bulk sludge, a distinguishing peak at 2430 cm^{-1} appeared on the membrane foulant which is related to the aminophosphonate group. Natural aminophosphonate groups are important source of nitrogen to bacteria and are biodegradable. However, equivalents used in industry are generally non-biodegradable (Huang et al., 2005). Thus, these groups, which are likely sourced from the oil refinery wastewater (e.g. dibutyl hydrogen phosphonate, as detailed in the motor oil ingredient) accumulated on the membrane surface (discussed in Section 3.2) through the process of adsorption, as they are known to have strong interaction with surfaces (Nowack, 2003). Similarly, as shown in Fig. 6, the FTIR bands at 1380 cm^{-1} are indicative of the —O—CO—CH_3 functional groups (hydrocarbon and carboxylic related). The intensity of the FTIR bands at this peak were distinctly high for the membrane foulant compared to the bulk sludge, which confirms that non-biodegradable hydrocarbon compounds derived from the influent wastewater are potential membrane foulants in MBR systems treating oil refinery wastewater.

3.5. Phylogenetic classifications in the MBR system and fouling implication

Microbial community composition of the anoxic sludge (ANS2 to 1), MBR sludge (AS3 to 1), and membrane foulants (MF3 to 1), was determined by high-throughput Illumina sequencing of the 16S rRNA genes to assess the contribution of membrane-adhered microorganisms to fouling development in the MBR system treating oil refinery wastewater. A total of 1,768,312 effective tags were obtained from all samples after raw tags were cleaned. Other characteristics of the pre-process sequencing data, quality control and sampling dates are summarized in the Table S1. New bacterial and archaeal phylotypes continue to emerge even after 25,000 sequencing reads, and thus shows that the sequencing depth for the samples library are sufficient to characterize the microbial communities (Fig. 7a). Similarly, the one-way pairwise analysis of similarity (ANOSIM) showed high semblance (R-value: −0.259) between duplicate samples. The sequence number of individual samples at each taxon level (Fig. 7b), and spread of the operational taxonomic units (OTUs) among all 24 samples (from 1900 to 3986 OTUs) are presented in Fig. S3.

Taxa abundance and alpha diversity indices of the 8 pooled samples using rarefied OTUs in terms of observed-species, Chao1, Shannon, ACE, Simpson, and goods-coverage are presented in Table 3. All the indices except for the goods-coverage (which indicate that the gene libraries comprise representative amount (>0.9) of the total sequences present in all samples), demonstrate that the bacterial community structure of mixed liquor samples (ANS and AS) are dissimilar to the membrane foulant samples, in terms of distribution and evenness as also reported by Matar et al. (2017). However, colonization of the membrane surface by microorganisms occurred in succession (MF3 to 1) with older biofoulant population being more diverse than earlier ones (as revealed by observed-species, Chao1, and ACE indices) except for Shannon index, which showed highest diversity for MF2 (Table 3). A different trend was observed for the mixed liquor samples (ANS and AS), as there was temporary decline in microbial diversity probably due to shock loading effect but subsequently increased as the biomass acclimatized (Table 3).

To verify if the bacterial communities in the mixed liquors are similar to the membrane foulant communities, NMDS plot was used for the visualization (Fig. 8a). Results showed that the bacterial communities in the mixed liquors from the middle to early stage (AS2 to 1 and ANS2 to 1) differs from the membrane foulant communities (MF2 to 1), but tend to form clusters relative to the sampling compartment. However, membrane foulants and mixed liquor samples retrieved on separate days with respect to influent concentration and TMP rises each formed clustered (Fig. 8a). Moreover, clustering of the bacterial communities in all samples were compared using the unweighted pair group method with arithmetic mean (UPMGA) to derive information about the dissimilarities among the samples (Fig. 8b). Although results from the NMDS plot showed that samples from different fouling episode clustered together, comparison of the unweighted Uni-Frac distance between samples in each categories revealed that late foulant microbial communities (MF1 and 2) are dissimilar from the early foulant communities (MF3). Matar et al. (2017), indicated that transfer of biomass community from mixed liquor to membrane surface was unlikely to shape the community structure on membrane surfaces but instead, species selection by biotic, abiotic, and local environmental conditions are responsible for selective migration of microorganism from activated sludge to membrane surfaces. As discussed in Sections 3.2 and 3.4, the membrane-fouling rate increased as the influent oil concentration increased. Thus, by implication, accumulation of organic macromolecules (e.g. emulsified oil) on the membrane surfaces can potentially alter the microbial community structure. However, clusters of microbial communities were observed at the same sampling period for anoxic (ANS1) and bulk (AS2) mixed liquor samples (Fig. 8b).

Among the 8 pooled samples, 13 dominant phylum and proteobacterial classes with taxa abundance >0.5% were assigned to the mixed liquor and membrane foulant samples. Dominant phylum in all 8 samples include *Proteobacteria* (52.1%) {*Gammaproteobacteria* (31.7%) > *Betaproteobacteria* (12.6%) > *Alphaproteobacteria* (5.0%) > Other *Proteobacteria* (1.7%) > Epsilonproteobacteria (1.1%) > *Actinobacteria* (12.5%) > *Bacteroidetes* (11.1%) > *Firmicutes* (6.1%) > *Acidobacteria* (4.3%) > *Planctomycetes* (2.61%) *Chloroflexi* (2.6%) > *Nitrospirae* (1.9%) > *Thermomicrobia* (1.4%) > *Gemmatimonadetes* (1.2%) > *Chlorobi* (0.74%) > *Verrucomicrobia* (0.73%) (Fig. S4). Among the proteobacterial classes, the class *Gammaproteobacteria* was relatively more dominant in the MF samples compared to the rest of the samples, while the highest percentage (43.9%) was observed in late foulant samples (MF1) relative to earlier MF samples (MF3). *Actinobacteria and Bacteroidetes* were the other dominant phyla observed across all the samples. *Actinobacteria* have been identified as efficient hydrocarbon degraders (Yu et al., 2018), and are common dominant phyla observed in activated sludge and MBR (Matar et al., 2017). However, to assess the variation of community structure on the

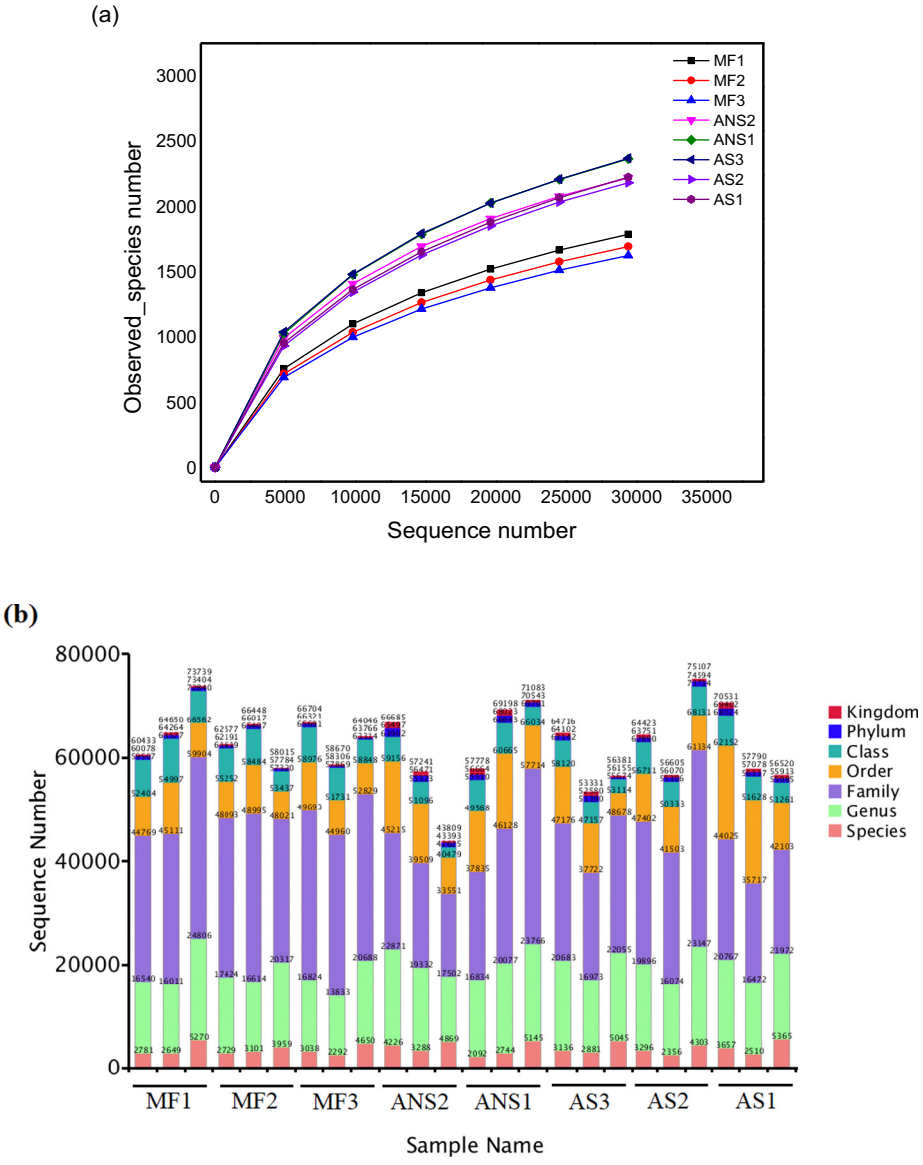

Fig. 7. (a) Taxa annotation including sequencing depth for the samples library (b) number of sequences at each taxonomic level.

membrane surface relative to the mixed liquors, assemblages of core genera (shared genera across each sample grouping i.e. MF, AS, and ANS) in the A/O-MBR were analyzed. Among the observed genera, only 380, 427, and 442 core genera respectively for membrane foulant, MBR, and anoxic sludge were shared among each sample grouping (Table 4). This resulted in approximately 20%, 10%, and 15% of genera in MF, AS and ANS, respectively that are dissimilar within the sampling compartment. However, of the 28 genera with relative abundance >0.5%, 12 core genera were shared across all 8 pooled samples. Six genera were shared between MF or AS and AS or ANS group, and 10 genera were unique to the entire group (i.e. 5 unique genera were observed in AS group, 4 in MF group and 1 in ANS group) (Fig. 9).

Among the MF subgrouping, certain genera including Aquicella, *Pseudomonas*, *Comamonas*, *Holophaga*, *Lactobacillus*, and the family

Table 3
Summary of the A/O-MBR microbial alpha diversity and taxa abundance.

Sample	No. of Phyla	Bacterial taxa abundance (%)	Archaeal taxa abundance (%)	Unclassified taxa (%)	Observed-species	Chao1	Shannon	ACE	Simpson	Goods-coverage
MF1	43	99.4	0.04	0.56	1790.3 ± 209.8	2411.9 ± 241.5	7.01 ± 0.48	2518.9 ± 260.7	0.96 ± 0.01	0.98 ± 0.003
MF2	40	99.4	0.08	0.56	1697.0 ± 322.4	2354.4 ± 494.3	7.08 ± 0.46	2435.2 ± 517.5	0.96 ± 0.01	0.98 ± 0.005
MF3	38	99.4	0.07	0.57	1628.3 ± 248.4	2275.3 ± 315.5	6.91 ± 0.53	2358.9 ± 353.2	0.96 ± 0.01	0.98 ± 0.004
ANS1	40	98.4	0.20	1.37	2220.3 ± 240.3	2884.7 ± 488.5	8.45 ± 0.10	3041.5 ± 483.4	0.99 ± 0.001	0.97 ± 0.005
ANS2	44	98.4	0.11	1.48	2366.7 ± 385.2	3175.4 ± 611.8	8.31 ± 0.17	3304.9 ± 607.6	0.99 ± 0.001	0.97 ± 0.007
AS1	46	99.0	0.08	0.91	2369.7 ± 545.2	3182.5 ± 660.2	8.43 ± 0.29	3293.8 ± 710.6	0.99 ± 0.002	0.97 ± 0.006
AS2	41	99.0	0.09	0.90	2184.7 ± 352.2	3047.9 ± 514.1	7.75 ± 0.09	3141.5 ± 620.0	0.97 ± 0.002	0.97 ± 0.006
AS3	45	98.4	0.25	1.30	2226.7 ± 184.2	3163.1 ± 244.9	8.17 ± 0.27	3290.1 ± 321.8	0.99 ± 0.005	0.97 ± 0.004

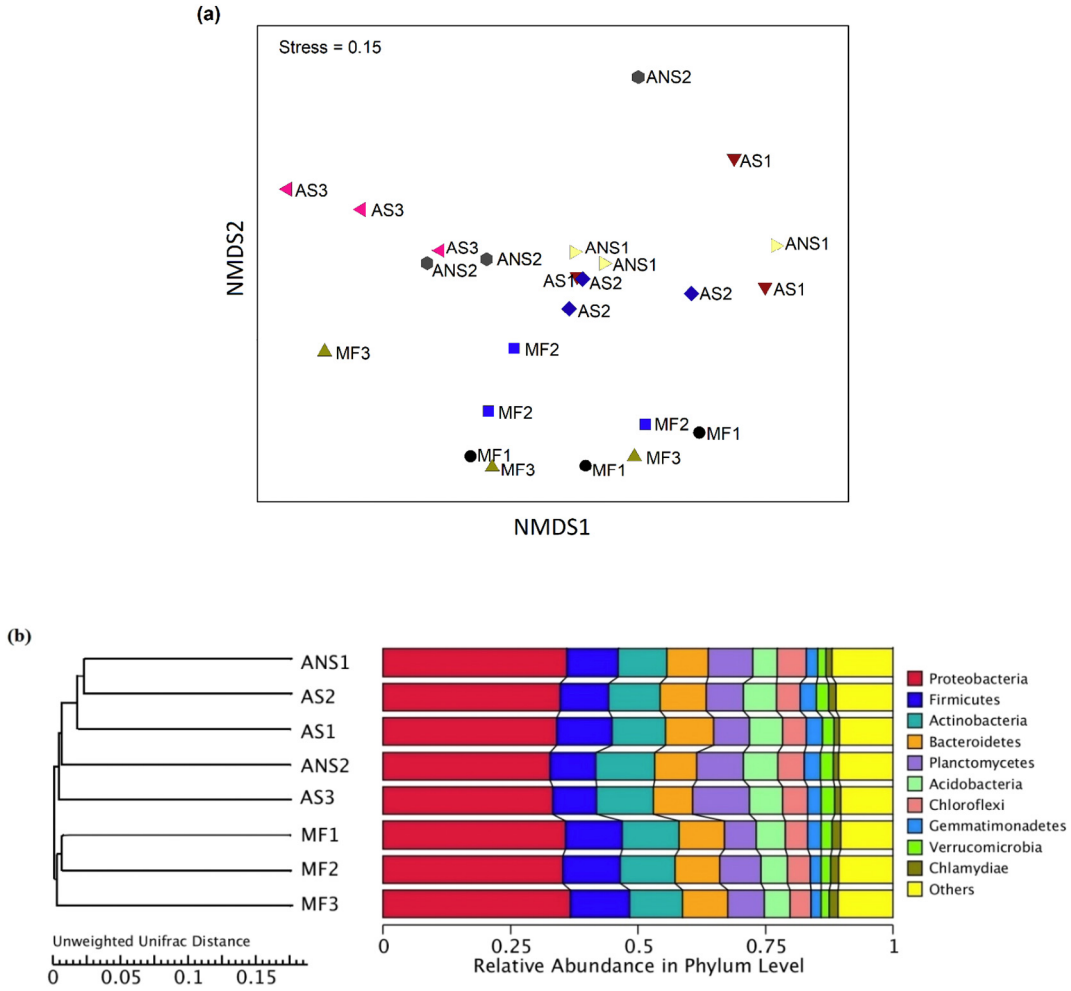

Fig. 8. Unweighted UniFrac distance based on (a) Nonmetric multidimensional scaling (NMDS) plot of the 8 pooled samples showing the different sampling subcategories i.e. membrane foulants (MF3-1), MBR mixed liquor (AS3-1) and anoxic sludge mixed liquor (ANS2-1). (b) Unweighted pair group method with arithmetic mean (UPGMA) clustering tree (On the left is the UPGMA cluster tree structure, and on the right is the species relative abundance distribution at the phylum level for each sample).

Chitinophagaceae, which belong to class Gammaproteobacteria, Betaproteobacteria, Holophagae, Bacilli, and the phylum Bacteroidetes, respectively were dominantly observed compared to other subgrouping (i.e. AS and ANS) (Fig. 9). These genera are known to thrive well in hydrocarbon rich environment and have been correlated with periods relating to high volumetric loading (Xia et al., 2010) with the increase production of EPS content, which facilitate the easy attachment of EPS-degrading (mainly polysaccharide) bacteria (e.g. Chitinophagaceae) to the membrane surface (Larsbrink et al., 2017). Furthermore, Roy et al. (2018), indicated that some members of Firmicutes, Gammaproteobacteria, Deltaproteobacteria, Epsilonproteobacteria, Betaproteobacteria and Bacteroidetes have been most frequently reported from petroleum hydrocarbon associated sites. As previously discussed in Sections 3.2 and 3.4, as influent loading rate increase, accumulation of hydrocarbon compounds were observed on the membrane surface most especially on Day 50 (MF1 samples). This scenario enhanced the selective growth of some hydrocarbon utilizing community including the genera *Comamonas* and *Lactobacillus* on the membrane surface (Fig. 9). *Comamonas* belonging to the order Burkholderiales and members of the family Enterobacteriaceae were shown to express assemblages of superior metabolic properties with ability to utilize polyaromatic and aliphatic (C_6 – C_{22}) compounds, and have been shown to be excellent degraders of total petroleum hydrocarbon (TPH) with multiple terminal electron acceptors (Sarkar et al., 2017).

In a similar finding, *Proteobacteria* genera derived from native oil refinery sludge showed decrease in the relative abundance of *Pseudomonas* (partially) and *Dechloromonas* with corresponding increase in *Bacillus* due to bioaugmentation (with native oil refinery sludge) and biostimulation (with nitrogen and phosphosrus) (Roy et al., 2018). Besides, the high clustering of *Rhodanobacter* in MF1, relative to MF2, MF3 and the mixed liquor samples suggest the availability of nitrate, which serves as biostimulant for the proliferation of the *Burkholderiales* members coupled with their ability to adapt in metal-stressed environment. The presence of relatively high abundance of phenol degraders including *Holophaga* and *Comamonas* on the membrane surface compared to the mixed liquors further confirms that aromatic and hydrocarbon compounds are main membrane foulants (Liesack et al., 1994; Zámocký et al., 2001). These results suggest that membrane surface colonizers during oil refinery wastewater treatment are not just a random

Table 4
Analysis of shared genera across each sample grouping (i.e. MF, AS, ANS).

Combined samples[a]	Average no. of observed genera[b]	No. of shared genera	% Age of shared genera
MF	473	380	80.3
AS	520	427	90.2
ANS	519	442	85.2

[a] Corresponds to combined samples (from Day 37, 43 and 50) for MF and AS samples, respectively and Day 37 and 43, for ANS samples.
[b] The average number of observed genera present in each of the sample groupings (i.e. MF, AS and ANS).

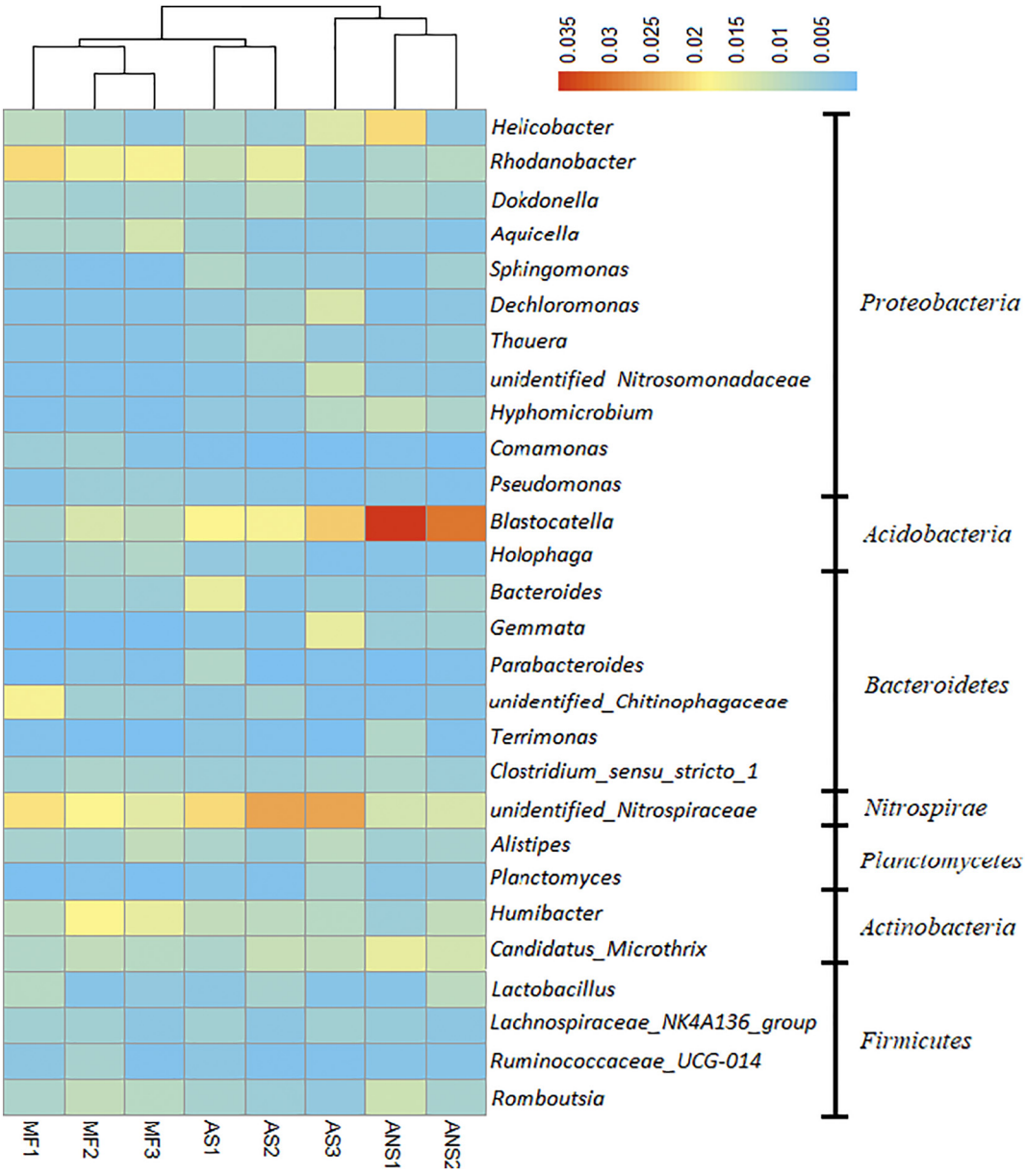

Fig. 9. Clustered heatmap distribution of the most abundant shared and unique genera among each category (i.e. MF, AS and ANS) of the 8 pooled samples with relative abundance >0.5%. The color scale represents the percentage of genus, which range from 0.5 to 3.5% in the corresponding samples.

migration of species from MBR bulk sludge (AS), but as a result preferred selection of species due to existing environmental condition.

4. Conclusion

In this study, we showed that emulsified oil with droplet sizes >0.5 μm are potential foulants in MBR, while concentration of chemical elements (Si, Fe, Al, Ce, Ba, Sr etc.) at membrane interface by complex interactions with EPS fractions (53.8 mg/g VSS) produced at high ORW volumetric loading (~18.7 kg COD/m^3/d) are inextricably linked with membrane fouling in the MBR system. Accumulation of ORW-derived less biodegradable organophosphonates and phenolic compounds on the membrane surface resulted in relatively high abundance of hydrocarbon and phenol degraders like *Lactobacillus*, *Comamonas*, and *Holophaga* at the membrane surface effecting a shift in microbial community structure of foulants in the MBR system. Conclusively, this work reveals that major membrane foulants in MBR system during oil refinery wastewater treatment are derived from the ORW influent, and can induce changes in microbial communities that are responsive to dynamic environment changes in the MBR system.

Acknowledgements

This work was supported by funds from the Bureau of Frontier Sciences and Education (QYZDB-SSW-DQC044), the Bureau of International Cooperation (132C35KYSB20160018), CAS, and the Chinese Academy of Sciences–The World Academy of Sciences (CAS-TWAS) president's fellowship program for developing countries. The technical assistance of Mrs. Gloria Oyagha is gratefully acknowledged.

Appendix A. Supplementary data

Supplementary data to this article can be found online at https://doi.org/10.1016/j.scitotenv.2018.06.049.

References

Abass, O., Wu, X., Guo, Y., Zhang, K., 2015. Membrane bioreactor in China: a critical review. Int. J. Membr. Sci. Technol. 2, 29–47.

Abass, O.K., Zhuo, M., Zhang, K., 2017. Concomitant degradation of complex organics and metals recovery from fracking wastewater: roles of nano zerovalent iron initiated oxidation and adsorption. Chem. Eng. J. 328, 159–171.

Alexandre, V.M.F., de Castro, T.M.S., de Araújo, L.V., Santiago, V.M.J., Freire, D.M.G., Cammarota, M.C., 2016. Minimizing solid wastes in an activated sludge system treating oil refinery wastewater. Chem. Eng. Process. Process Intensif. 103, 53–62.

An, C., Huang, G., Yao, Y., Zhao, S., 2017. Emerging usage of electrocoagulation technology for oil removal from wastewater: a review. Sci. Total Environ. 579, 537–556.

APHA, 2005. Standard Methods for the Examination of Water and Wastewater. twentieth ed. American Public Health Association, American Water Works Association, Water Environmental Federation, Washington, USA.

Ben-Youssef, C., Vazquez-Rodriguez, G.A., 2011. Model-based design of different fedbatch strategies for phenol degradation in acclimatized activated sludge cultures. Bioresour. Technol. 102, 3740–3747.

Boyer, A., Ning, P., Killey, D., Klukas, M., Rowan, D., Simpson, A.J., et al., 2018. Strontium adsorption and desorption in wetlands: role of organic matter functional groups and environmental implications. Water Res. 133, 27–36.

Caporaso, J.G., Kuczynski, J., Stombaugh, J., Bittinger, K., Bushman, F.D., Costello, E.K., et al., 2010. QIIME allows analysis of high-throughput community sequencing data. Nat. Methods 7, 335–336.

Chen, J., Zhang, M., Li, F., Qian, L., Lin, H., Yang, L., et al., 2016. Membrane fouling in a membrane bioreactor: high filtration resistance of gel layer and its underlying mechanism. Water Res. 102, 82–89.

Di Fabio, S., Malamis, S., Katsou, E., Vecchiato, G., Cecchi, F., Fatone, F., 2013. Are centralized MBRs coping with the current transition of large petrochemical areas? A pilot study in Porto-Marghera (Venice). Chem. Eng. J. 214, 68–77.

Fakhru'l-Razi, A., Pendashteh, A., Abdullah, L.C., Biak, D.R., Madaeni, S.S., Abidin, Z.Z., 2009. Review of technologies for oil and gas produced water treatment. J. Hazard. Mater. 170, 530–551.

Golub, A., Piekutin, J., 2018. Use of porous materials to remove oil contaminants from water. Sci. Total Environ. 627, 723–732.

Hong, H., Zhang, M., He, Y., Chen, J., Lin, H., 2014. Fouling mechanisms of gel layer in a submerged membrane bioreactor. Bioresour. Technol. 166, 295–302.

Huang, J., Su, Z., Xu, Y., 2005. The evolution of microbial phosphonate degradative pathways. J. Mol. Evol. 61, 682–690.

Koehler, L.H., 1952. Differentiation of carbohydrates by anthrone reaction rate and color intensity. Anal. Chem. 24, 1576–1579.

Larsbrink, J., Tuveng, T.R., Pope, P.B., Bulone, V., Eijsink, V.G., Brumer, H., et al., 2017. Proteomic insights into mannan degradation and protein secretion by the forest floor bacterium *Chitinophaga pinensis*. J. Proteome 156, 63–74.

Liesack, W., Bak, F., Kreft, J.-U., Stackebrandt, E., 1994. *Holophaga foetida* gen. nov., sp. nov., a new, homoacetogenic bacterium degrading methoxylated aromatic compounds. Arch. Microbiol. 162, 85–90.

Lin, H., Liao, B.Q., Chen, J., Gao, W., Wang, L., Wang, F., et al., 2011. New insights into membrane fouling in a submerged anaerobic membrane bioreactor based on characterization of cake sludge and bulk sludge. Bioresour. Technol. 102, 2373–2379.

López, J., Imperial, S., Valderrama, R., Navarro, S., 1993. An improved Bradford protein assay for collagen proteins. Clin. Chim. Acta 220, 91–100.

Magoc, T., Salzberg, S.L., 2011. FLASH: fast length adjustment of short reads to improve genome assemblies. Bioinformatics 27, 2957–2963.

Matar, G.K., Bagchi, S., Zhang, K., Oerther, D.B., Saikaly, P.E., 2017. Membrane biofilm communities in full-scale membrane bioreactors are not randomly assembled and consist of a core microbiome. Water Res. 123, 124–133.

Meng, F., Zhang, S., Oh, Y., Zhou, Z., Shin, H.S., Chae, S.R., 2017. Fouling in membrane bioreactors: an updated review. Water Res. 114, 151–180.

Munirasu, S., Haija, M.A., Banat, F., 2016. Use of membrane technology for oil field and refinery produced water treatment—a review. Process. Saf. Environ. Prot. 100, 183–202.

Nowack, B., 2003. Environmental chemistry of phosphonates. Water Res. 37, 2533–2546.

Padaki, M., Surya Murali, R., Abdullah, M.S., Misdan, N., Moslehyani, A., Kassim, M.A., et al., 2015. Membrane technology enhancement in oil–water separation. A review. Desalination 357, 197–207.

Pajoumshariati, S., Zare, N., Bonakdarpour, B., 2017. Considering membrane sequencing batch reactors for the biological treatment of petroleum refinery wastewaters. J. Membr. Sci. 523, 542–550.

Qin, L., Fan, Z., Xu, L., Zhang, G., Wang, G., Wu, D., et al., 2015. A submerged membrane bioreactor with pendulum type oscillation (PTO) for oily wastewater treatment: membrane permeability and fouling control. Bioresour. Technol. 183, 33–41.

Rahman, M.M., Al-Malack, M.H., 2006. Performance of a crossflow membrane bioreactor (CF–MBR) when treating refinery wastewater. Desalination 191, 16–26.

Razavi, S.M.R., Miri, T., 2015. A real petroleum refinery wastewater treatment using hollow fiber membrane bioreactor (HF-MBR). J. Water Process Eng. 8, 136–141.

Roy, A., Dutta, A., Pal, S., Gupta, A., Sarkar, J., Chatterjee, A., et al., 2018. Biostimulation and bioaugmentation of native microbial community accelerated bioremediation of oil refinery sludge. Bioresour. Technol. 253, 22–32.

Santo, C.E., Vilar, V.J.P., Botelho, C.M.S., Bhatnagar, A., Kumar, E., Boaventura, R.A.R., 2012. Optimization of coagulation–flocculation and flotation parameters for the treatment of a petroleum refinery effluent from a Portuguese plant. Chem. Eng. J. 183, 117–123.

Santos, B., Crespo, J.G., Santos, M.A., Velizarov, S., 2016. Oil refinery hazardous effluents minimization by membrane filtration: an on-site pilot plant study. J. Environ. Manag. 181, 762–769.

Sarkar, P., Roy, A., Pal, S., Mohapatra, B., Kazy, S.K., Maiti, M.K., et al., 2017. Enrichment and characterization of hydrocarbon-degrading bacteria from petroleum refinery waste as potent bioaugmentation agent for in situ bioremediation. Bioresour. Technol. 242, 15–27.

Shariati, S.R., Bonakdarpour, B., Zare, N., Ashtiani, F.Z., 2011. The effect of hydraulic retention time on the performance and fouling characteristics of membrane sequencing batch reactors used for the treatment of synthetic petroleum refinery wastewater. Bioresour. Technol. 102, 7692–7699.

Socrates, G., 1980. Infrared Characteristic Group Frequencies. Wiley, New York.

USEPA, 2009. Method 1664 A: n-Hexane Extractable Material (HEM; Oil and Grease) and Silica Gel n-Hexane Extractable Material (SGT-HEM; Non-Polar Material) by Extraction and Gravity. EPA, USA.

Viero, A., Demelo, T., Torres, A., Ferreira, N., Santannajr, G., Borges, C., et al., 2008. The effects of long-term feeding of high organic loading in a submerged membrane bioreactor treating oil refinery wastewater. J. Membr. Sci. 319, 223–230.

Volkov, I.V., Polyakov, E.V., Denisov, E.I., Ioshin, A.A., 2017. Sorption behavior of strontium ions in humic acid solutions. Radiochemistry 59, 70–78.

Wang, Q., Garrity, G.M., Tiedje, J.M., Cole, J.R., 2007. Naive Bayesian classifier for rapid assignment of rRNA sequences into the new bacterial taxonomy. Appl. Environ. Microbiol. 73, 5261–5267.

Wang, Z., Tang, S., Zhu, Y., Wu, Z., Zhou, Q., Yang, D., 2010. Fluorescent dissolved organic matter variations in a submerged membrane bioreactor under different sludge retention times. J. Membr. Sci. 355, 151–157.

Wang, Y., Wang, Q., Li, M., Yang, Y., He, W., Yan, G., et al., 2016. An alternative anaerobic treatment process for treatment of heavy oil refinery wastewater containing polar organics. Biochem. Eng. J. 105, 44–51.

Wang, B.B., Liu, X.T., Chen, J.M., Peng, D.C., He, F., 2017. Composition and functional group characterization of extracellular polymeric substances (EPS) in activated sludge: the impacts of polymerization degree of proteinaceous substrates. Water Res. 129, 133–142.

Wu, J., Le-Clech, P., Stuetz, R.M., Fane, A.G., Chen, V., 2008. Effects of relaxation and backwashing conditions on fouling in membrane bioreactor. J. Membr. Sci. 324, 26–32.

Xia, S., Li, J., He, S., Xie, K., Wang, X., Zhang, Y., et al., 2010. The effect of organic loading on bacterial community composition of membrane biofilms in a submerged polyvinyl chloride membrane bioreactor. Bioresour. Technol. 101, 6601–6609.

Xin, Y., Bligh, M.W., Kinsela, A.S., Wang, Y., David Waite, T., 2015. Calcium-mediated polysaccharide gel formation and breakage: impact on membrane foulant hydraulic properties. J. Membr. Sci. 475, 395–405.

Xu, X., Cho, S.I., Sammel, M., You, L., Cui, S., Huang, Y., et al., 1998. Association of petrochemical exposure with spontaneous abortion. Occup. Environ. Med. 55, 31–36.

Xu, J., Sheng, G.P., Ma, Y., Wang, L.F., Yu, H.Q., 2013. Roles of extracellular polymeric substances (EPS) in the migration and removal of sulfamethazine in activated sludge system. Water Res. 47, 5298–5306.

Yu, S., Mei, H., Chen, X., Tan, X., Ahmad, B., Alsaedi, A., et al., 2015. Impact of environmental conditions on the sorption behavior of radionuclide 90Sr(II) on Na-montmorillonite. J. Mol. Liq. 203, 39–46.

Yu, L., Yang, Y., Yang, B., Li, Z., Zhang, X., Hou, Y., et al., 2018. Effects of solids retention time on the performance and microbial community structures in membrane bioreactors treating synthetic oil refinery wastewater. Chem. Eng. J. 344, 462–468.

Yuan, S.J., Sun, M., Sheng, G.P., Li, Y., Li, W.W., Yao, R.S., et al., 2011. Identification of key constituents and structure of the extracellular polymeric substances excreted by Bacillus megaterium TF10 for their flocculation capacity. Environ. Sci. Technol. 45, 1152–1157.

Zámocký, M., Godočíková, J., Koller, F., Polek, B., 2001. Potential application of catalase-peroxidase from *Comamonas terrigena* N3H in the biodegradation of phenolic compounds. Antonie Van Leeuwenhoek 79, 109–117.

Zhang, X., Wang, Z., Wu, Z., Wei, T., Lu, F., Tong, J., et al., 2011. Membrane fouling in an anaerobic dynamic membrane bioreactor (AnDMBR) for municipal wastewater treatment: characteristics of membrane foulants and bulk sludge. Process Biochem. 46, 1538–1544.